JOURNAL OF Applied Polymer SCIENCE

Preparation of Microcellular Thermoplastic Elastomer Foams from Polystyrene-*b*-ethylene-butylene-*b*-polystyrene (SEBS) and Their Blends with Polystyrene

Rahida Wati Binti Sharudin, Masahiro Ohshima
Department of Chemical Engineering, Kyoto University, Kyoto 615-8510, Japan
Correspondence to: M. Ohshima (E-mail: oshima@cheme.kyoto-u.ac.jp)

ABSTRACT: A microcellular foam was prepared from a thermoplastic elastomer by a batch physical foaming with CO_2. Two hydrogenated polystyrene-*b*-polybutadiene-*b*-polystyrene (SEBS) copolymers with different styrene ratios were used as an elastomer basis and blended with polystyrene (PS) to control their rigidity and gas permeability. The end-blocks of the SEBS form a physical cross-link and provide a rubber-like elasticity when cooled. SEBS alone, with its lower styrene content, cannot be physically foamed while retaining a stable-shape dimension because of its higher gas permeability and lower rigidity. SEBS with higher styrene contents were used, or the PS blend ratio was increased to 80/20 or 50/50, and batch physical foaming experiments were conducted at three temperature levels (60, 100, and 120°C) while the sorption CO_2 pressure was maintained at 10 MPa. Increasing the styrene content or blending PS with SEBS increased the storage modulus and decreased the gas permeability. As a result, the shrinkage of the foam was controlled, and stable microcellular elastomer foams could be prepared. © 2012 Wiley Periodicals, Inc. J. Appl. Polym. Sci. 000: 000–000, 2012

KEYWORDS: foam shrinkage; elastomer; elasticity; CO_2 diffusivity; entanglement

Received 7 February 2012; accepted 22 May 2012; published online
DOI: 10.1002/app.38104

INTRODUCTION

Recently, rubber foaming has been intensively studied by many researchers because of its great demand.[1–3] Chemical blowing agents (CBA) have typically been used for foaming rubbers. CBAs are chemicals that release a gas (such as CO_2 and N_2) when decomposed by heating. The released gas dissolves into the rubber or directly leads to bubble nucleation and the formation of a cellular structure in the rubber. The current major problem with the use of CBA in the foaming process is the emission of harmful substances and the contamination of foam products with residual CBA, which makes recycling difficult.

To solve the recycling issue, several researchers have conducted intensive studies on the physical foaming of rubbers and elastomers. They used nontoxic and lower global-warming-potential foaming agents, such as N_2 and CO_2, as physical blowing agents. For example, Kim et al.[4] studied the foamability of thermoplastic vulcanizates with various physical blowing agents (PBA). They reported that CO_2 was a good blowing agent to prepare lower density foams (high expansion foams), while N_2 was the best agent for preparing foams with a finer cell structure. Sahnoune et al.[5] prepared an elastomer foam using water as a nontoxic blowing agent.

When elastomers and rubbers were physically foamed, shrinkage and dimensional stability of the foam products became a critical issue. Rubbers are difficult to foam because they behave elastically and are less rigid. Sometimes, rigid fillers and short glass fibers are added to rubbers to reinforce their foams.[6] Vulcanization is commonly conducted to increase the rigidity and the stability of the foam. Vulcanization controls the chain mobility of rubber by introducing crosslinking agents, such as sulfur. Therefore, in rubber foaming with CBA, vulcanization and CBA decomposition reactions must be simultaneously controlled to retain both the viscoelastic properties of rubber and the gas liberation rate at appropriate levels. The compounding technique and the vulcanization conditions affect the parameters of the final cellular structure, such as the cell size, cell density, and cell uniformity. For example, when the vulcanization reaction proceeds faster than the gas liberation rate, cell growth is prevented, and higher expansion foam is not obtained. When the gas liberation rate proceeds faster than the vulcanization reaction rate, the foam is not stabilized. There have been many reports on rubber foaming with vulcanization.[7–9] Tai et al.[10] investigated the effect of the crosslink density of a metallocene elastomer (m-POE) by varying the loading of the cross linking agent. Ariff et al.[11] reported that rubbers with higher degrees of

crosslink density produce stiffer cell walls and provide greater restriction to expansion.

As a substitute technique for vulcanization, high-energy irradiation techniques have been proposed for the production of cross linked networks.[12–16] The technique has attracted attention because it is fast and clean, it requires less energy and it has the potential to improve chemical resistance.[17] Liu et al.[14] used the irradiation cross linking technique to control the physical and mechanical properties of silicone rubber foam. Dubey et al.[15] reported that a significant improvement in the mechanical properties of an Styrene-butadiene rubber (SBR)-Ethylene propylene diene rubber (EPDM) blend was achieved by the irradiation technique. However, the use of this technique has been restricted because high energy radiation is hazardous to human health[18]; furthermore, the technique is not applicable to certain polymers because of their poor resistance against radiation and poor impact resistance at low temperature.[19]

Because of vulcanization and the residual CBA, most elastomer or rubber foams are difficult to recycle. Thermoplastic elastomers (TPE), often called thermoplastic rubbers, are a class of copolymers or physical mixes of polymers (usually a plastic and a rubber) that possess both thermoplastic and elastomeric properties. Therefore, TPEs have advantages of both rubbery and plastic materials. The crosslinking in TPE is a weaker dipole or hydrogen bond, which is debonded by heating, while the crosslink created during the vulcanization of a rubber or elastomer is a covalent bond. These properties make TPEs recyclable; consequently, they are suitable for recyclable microcellular rubber foams. Although great success has been made in the production of microcellular foams from thermoplastic polymers, a limited number of reports have been made on microcellular TPE foams. Zhai et al.[20] prepared microcellular poly(ethylene-*co*-octene) (PEOc) foam using CO_2 as a physical blowing agent and reported that the increase of the PEOc molecular weight increased the matrix modulus and melt viscosity and tended to stabilize the cell structure at high foaming temperatures.

In this study, hydrogenated polystyrene-*b*-polybutadiene-*b*-polystyrene (SEBS) was investigated for physical foaming with CO_2. SEBS is a type of TPE that consists of a soft midblock of ethylene–butylene (EB) and hard polystyrene end-blocks. The end-blocks (styrene) form a physical crosslink and provide a rubber-like elasticity. With the increase of styrene block percentage, the storage modulus and melt viscosity can be increased, and the diffusivity of CO_2 can be decreased. Two SEBS with different styrene contents were foamed at three different foaming temperatures to determine the effect of the styrene content on the microcellular structure. Furthermore, because SEBS has good compatibility with polystyrene (PS), PS can be used to tune the modulus and diffusivity of CO_2 by blending. The effects of physical crosslinking and the blend ratio of PS on the rheological properties and the cellular structure are examined in this study.

EXPERIMENTAL

Material

Two SEBS copolymers with different styrene contents (H1062 and H1043) were kindly provided by Asahi Kasei Elastomer. H1062 is composed of 18 wt % styrene blocks and 82 wt % ethylene–butylene blocks, and its average molecular weight is 70,000 g mol^{-1}. H1043 possesses a higher styrene content of 67 wt %, an EB content of 33 wt % and a molecular weight of 45,000. Polystyrene (PS) (M_w = 192,000 g mol^{-1}, Aldrich) was also used as received.

Experimental

Blend Sample Preparation. SEBS/PS blend samples were prepared at two different blend ratios, 80/20 and 50/50. The blending was conducted by a twin-screw extruder (ULT nano05, TECHNOVEL, Japan). The screw rotation speed was kept constant at 38 rpm during the blending process. The barrel temperature of the extruder was set at 200, 210, and 220°C for the solid conveying, compression, and metering sections. The extrudate was cut into small pieces and compression-molded into rectangular samples that were 2 mm in diameter, 3 mm in length, and 1 mm in thickness using a hot press (SS, Imoto Seisakusho, Japan) at 220°C and 20 MPa for 10 min.

Solubility and Diffusivity Measurements. A magnetic suspension balance (MSB; Robotherm and Bel Japan) was used to measure the solubility and diffusivity of CO_2 in two SEBS copolymers and their PS blends. When CO_2 dissolves in a polymer, the weight of the polymer increases because of the weight of the dissolved CO_2. Thus, weighing the polymer under pressurized CO_2 allows us to determine the solubility and diffusivity of CO_2. The MSB makes it possible to weigh samples under high pressures and temperatures. The details of this measurement scheme are described elsewhere.[21] When CO_2 dissolves in the polymer, it causes the polymer to swell. Because the buoyancy caused by the swelling affects the solubility measurements, the specific volume of the polymer/CO_2 mixture must be estimated accurately to conduct a correction of buoyancy and obtain the true transport properties. The specific volume at a given temperature and pressure was calculated by the Sanchez-Lacombe equation of state (S-L EOS) and a mixing rule with a binary interaction parameter, k_{12}.[21,22] The characteristic parameters of the S-L EOS for each polymer blend were determined from the Pressure–Volume–Temperature (PVT) data (Figure 1). The resulting parameter values are listed in Table I. The solubility of CO_2 in PS, SEBS and their blends was measured at pressures ranging from 5 to 18 MPa. CO_2 of 99.9% purity (Showa Tansan, Japan) was used.

To estimate the specific volume of polymer/CO_2 single phase mixture, the Sanchez-Lacombe equation of state (SL EOS) was used in the following way.

The SL-EOS was derived from a lattice model to describe the relationship among the specific volume (density), pressure, and temperature and it is given by

$$\tilde{\rho}^2 + \tilde{P} + \tilde{T}\left[\ln(1-\tilde{\rho}) + \left(1 - \frac{1}{r}\right)\tilde{\rho}\right] = 0 \qquad (1)$$

where $\tilde{T}, \tilde{P}$, and $\tilde{\rho}$ are the reduced temperature, pressure and density, respectively. r is the size parameter, which represents the number of lattice sites occupied by one polymer chain.

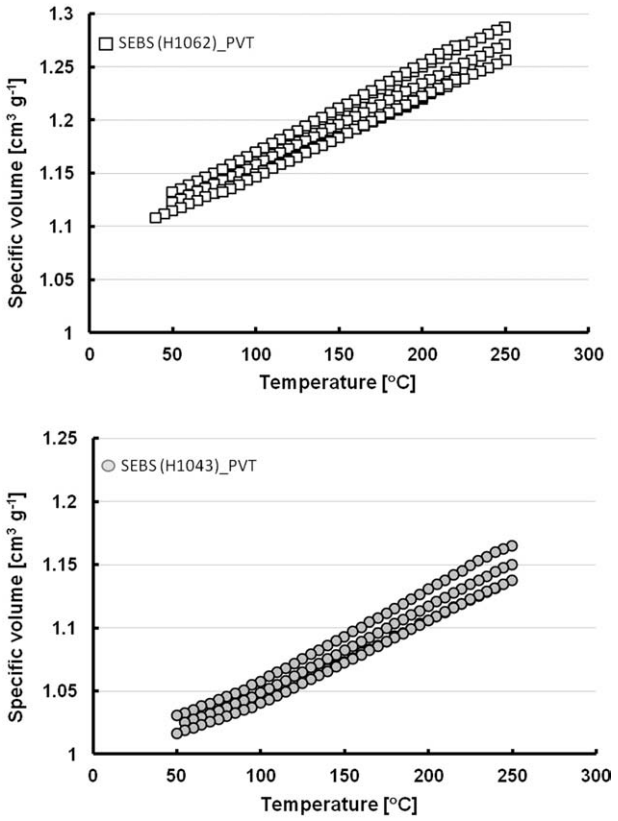

Figure 1. Measured PVT data of SEBS (H1062) and SEBS (H1043).

The reduced parameters and size parameter are defined by

$$\tilde{P} = \frac{P}{P^*}, \tilde{\rho} = \frac{\rho}{\rho^*}, \tilde{T} = \frac{T}{T^*}, r = \frac{P^*}{RT^*}\left(\frac{\bar{M}_w}{\rho^*}\right), v^* = T^*\frac{R}{P^*} \quad (2)$$

where R is the gas constant and $\bar{M}_w$ is the weight average molecular weight, and P^*, T^*, v^*, and ρ^* are characteristic parameters.

When the SL equation of state is used for a single component, such as for neat polymer or CO_2 alone, the characteristic parameters can be obtained either from the literature or by fitting eq. (1) to PVT experimental data of the neat polymer or CO_2. To estimate the specific volume of a polymer blend/CO_2 mixture, a mixing rule is employed to modify the characteristic parameters in eq. (1) for blend system. The mixing rule used for our blend/CO_2 mixture was given by eqs. (3-1)–(3-8),[21,23–26] where the subscript 1 and 2 stand for parameters of CO_2 and polymer respectively.

$$P^* = \varphi_1 P_1^* + \varphi_2 P_2^* - \varphi_1\varphi_2\left(P_1^* + P_2^* - 2(1-k_{12})\left(P_1^* P_2^*\right)^{0.5}\right) \quad (3\text{-}1)$$

$$T^* = \frac{P^* v^*}{R} \quad (3\text{-}2)$$

$$v^* = \varphi_1^0 v_1^* + \varphi_2^0 v_2^* \quad (3\text{-}3)$$

$$\varphi_i^0 = \frac{\varphi_i}{\left(\varphi_i + \frac{v_1^*}{v_2^*}\varphi_2\right)} \quad (3\text{-}4)$$

Table I. Characteristic Parameters of the Sanchez-Lacombe Equation of State

	H1062	H1043	PS	H1062/PS			H1043/PS		
				80/20	50/50	80/20	50/50		
T^* (K)	6.5599E + 02	6.7455E + 02	6.9512E + 02	6.5209E + 02	6.7335E + 02	6.9216E + 02	6.9512E + 02		
P^* (K)	3.1685E + 08	3.4094E + 08	3.1123E + 08	3.2507E + 08	3.1909E + 08	3.0777E + 08	3.1123E + 08		
ρ^* (kg/m^3)	9.3939E + 02	1.0319E + 02	1.0338E + 03	9.6967E + 02	1.0144E + 03	1.0338E + 03	1.0338E + 03		
M_w (kg/mol)	7,000	45,000	192,000	94,400	131,000	74,400	118,500		
k_{12}_62°C	0.1309	0.1299							
k_{12}_100°C	0.1349	0.1320	0.1266	0.1332	0.1351	0.1337	0.1317		
k_{12}_155°C	0.1412	0.1382	0.1526						
k_{12}_200°C	0.1523	0.1333							

M_w of blend was calculated by weight average of neat polymers.

$$\rho^* = \frac{1}{\left(\frac{m_1}{\rho_1^*} + \frac{m_2}{\rho_2^*}\right)} \tag{3-5}$$

$$r = x_1 r_1 + (1 - x_1) r_2 \tag{3-6}$$

$$x_i = \frac{\left(\frac{W_i}{\bar{M}_{w,i}}\right)}{\left(\frac{W_i}{\bar{M}_{w,i}} + \frac{W_2}{\bar{M}_{w,2}}\right)} \tag{3-7}$$

$$\varphi_i = \frac{\left(\frac{m_i}{\rho_i^*}\right)}{\left(\frac{m_i}{\rho_i^*}\right) + \left(\frac{m_2}{\rho_2^*}\right)} \tag{3-8}$$

$$m_i = \frac{W_i}{W_i + W_2} \tag{3-9}$$

where T_i^*, P_i^*, ρ_i^* and $r_i$are characteristic parameters of ith component, W_i, $m_i$and x_i are weight, weight fraction and mole fraction of the ith component in the mixture, respectively and k_{ij} is the binary interaction parameter between the ith and the jth components.

An orthodox method of obtaining the SL EOS for the SEBS/PS/CO_2 system is to use the mixing rule regarding the system as a ternary system: the characteristic parameters of CO_2, SEBS, and PS are determined individually each PVT data. Then, two interaction parameters between polymers (SEBS and PS) and CO_2 are determined from MSB measurement of each polymer/CO_2 binary system. The third interaction parameter between SEBS and PS is determined by fitting eq. (1) to MSB measurement of SEBS/PS/CO_2 ternary systems with two predetermined interaction parameters of polymer/CO_2 binary systems. However, in this study, assuming that each SEBS/PS blend can be treated as one grade of polymer and SEBS/PS/CO_2 can be treated as a polymer/CO_2 binary system, we applied the following simple method for calculating the specific volume of mixtures of SEBS/PS/CO_2 with blend ratios of SEBS/PS at 80/20 and 50/50. Therefore, the characteristic parameters of SEBS/PS blend were determined by fitting eq. (1) to the PVT data of the blend. The molecular weight of the blend was determined by weight average of the molecular weight of SEBS and PS:

$$\bar{M}_w = m_1 \bar{M}_{w,1} + (1 - m_1) \bar{M}_{w,2} \tag{4}$$

where $\bar{M}_{w,1}$ and $\bar{M}_{w,2}$are the molecular weights of SEBS and PS, respectively.

Rheological Characterization. The linear dynamic storage modulus, G', was measured by a rheometer (ARES, TA Instrument Japan) at a strain of 0.1%. A dynamic temperature ramp test was also performed in a rectangular torsion mode in the temperature range from 30 to 120°C. The strain was maintained at 0.1% with a frequency of 1 rad s^{-1}. The heating rate was 2 °C min^{-1} for all tests. The frequency sweep test was also carried out at two different temperatures (60 and 100°C) with a fixed 0.1% strain in the frequency range from 0.1 to 100 $rads^{-1}$.

Foaming Experiment. Pressure quench batch foaming experiments were carried out with a high pressure autoclave equipped with pressure and temperature controllers. CO_2 was used as a physical blowing agent. After adsorption of CO_2 at 10 MPa at a desired temperature in 6 h, the pressure was released at a depression rate of approximately 1 $MPas^{-1}$ while the temperature was maintained.

Morphology Characterization. The cell morphology of the foamed samples was analyzed by a scanning electron microscope (SEM) (Tiny-SEM, Technex, Japan) after cryo-fracturing with liquid nitrogen and gold coating with 20 s of processing time. The solid and foam densities were measured using a densimeter (MP-200S, AlfaMirage, Japan).

RESULTS AND DISCUSSION

Solubility and Diffusivity of CO_2 in SEBS

Figures 2 and 3 show the solubility and diffusivity data, respectively, of CO_2 in the two SEBS copolymers in the range from 6 to 18 MPa and temperatures of 60, 100, and 155°C, which covers the foaming temperatures in this study. The resulting binary interaction parameters, k_{12}, are listed in Table I. In the given pressure range, the solubility of CO_2 in all polymers increases proportionally with CO_2 pressure and follows Henry's law. With the increase of the styrene content, the solubility decreased. Figure 3 plots the logarithmic mutual diffusion coefficient against the inverse of the temperature ($1/T$). The diffusion coefficients were calculated by taking the average values measured in the pressure range from 7 to 12 MPa.

The solubility increases and the diffusivity decreases as the temperature decreases in accordance with Henry's law. Furthermore, the diffusivity and solubility of CO_2 in SEBS (H1043) are lower than those in SEBS (H1062). The difference in the diffusivity of CO_2 between H1062 and H1043 is large, especially at the lower temperature of 62°C. Thus, the CO_2 permeability (which is the product of the solubility and the diffusivity) of SEBS (H1043) is lower than that of SEBS (H1062) at any investigated foaming temperature.

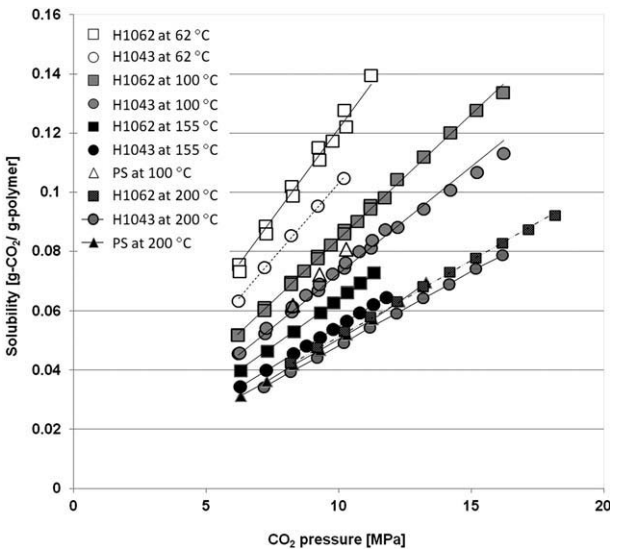

Figure 2. Solubility of CO_2 in PS, SEBS, and SEBS/PS blends at different temperatures.

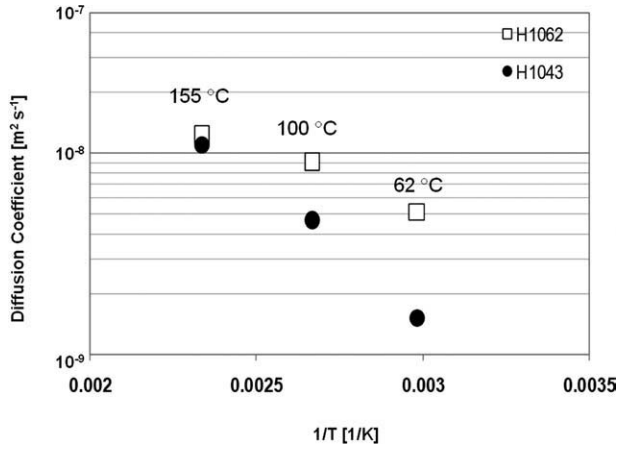

Figure 3. Temperature dependency of the diffusion coefficient of CO_2 in SEBS.

Figure 4 shows the solubility and diffusivity of CO_2 in the SEBS blends at a temperature of 100°C under 10 MPa CO_2 pressure. As the PS content increased in the H1043/PS blend, the diffusivity decreased and the solubility increased compared with those in neat H1043. This is because the solubility and diffusivity of CO_2 in PS is respectively higher and lower than that in the neat H1043.

The changes in the solubility and diffusivity were detectable at 20 wt % PS content in H1043/PS blend. However, for H1062/PS blends, the changes in the solubility and diffusivity at 20 wt % PS contents were too subtle to be differentiated from experimental measurement errors due to interaction (miscibility) between EB block of H1062 and PS. They became prominent when PS content was increased to 50 wt % in the blend. Considering the fact that both diffusivity and solubility of CO_2 in PS were lower than those in H1062 as shown in Figures 2 and 4, it is natural to speculate that the solubility and diffusivity of CO_2 in H1062/PS decreases with the increase of PS content in the blend. The permeability of the gas molecules is determined by the T_g of polymer. Low T_g rubbery polymers usually, need lower energy to create microcavity for gas molecules diffusion

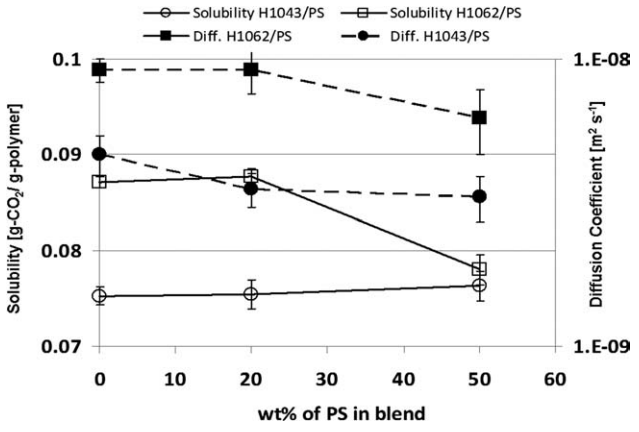

Figure 4. Solubility and diffusivity of CO_2 in polymer blends with different PS%.

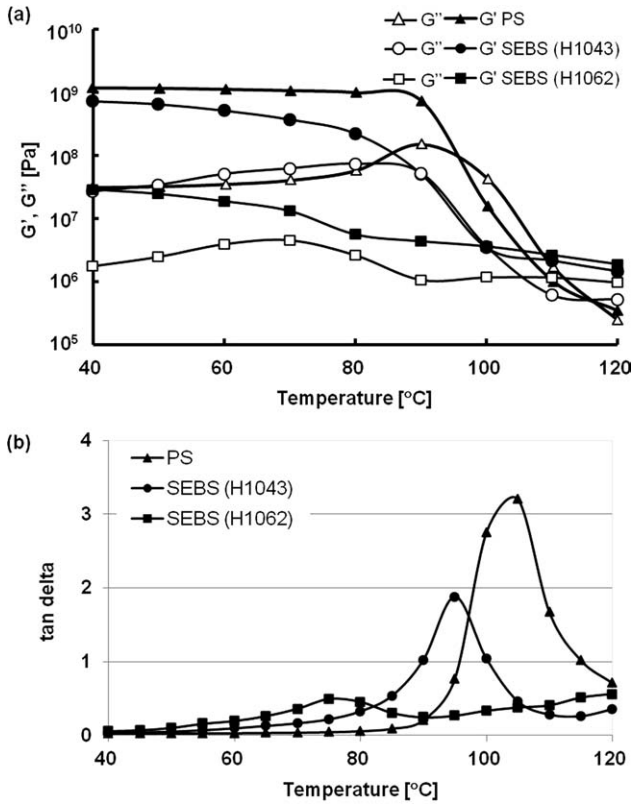

Figure 5. Rheological characterization of PS and SEBS: (a) G' and G'' of PS and SEBS and (b) tan delta of PS and SEBS.

as compared to high T_g glassy polymer.[27] By considering this fact, it could be speculated from our CO_2 diffusivity data that blending PS into SEBS could decrease the CO_2 permeability and thus, minimize the foam shrinkage.

Rheological Characterization

Figure 5(a) shows the temperature dependence of the storage modulus, G', and the loss modulus, G'', of PS and the two SEBS copolymers. The measurements were conducted at a strain of 0.1% and a frequency of 1 rad s^{-1}. These data indicate that the G' of PS is highest, that of SEBS (H1043) is second, and that of SEBS (H1062) is lowest in the temperature range from 40 to 100°C, which is below the T_g of polystyrene.

On the basis of the temperature at which tan δ shows the peak value, T_g values of PS, H1062 and H1043 are identified to be 105, 75, and 95°C, respectively as shown in Figure 5(b). Figures 6 and 7 show G' and G'', respectively, of the SEBS (H1062)/PS and SEBS (H1043)/PS blends with two different blend weight ratios, 80/20 and 50/50. Blending PS with SEBS (H1062) at 20 wt % reduced both G' and the absolute values of complex viscosity from those of neat PS. At temperatures below 80°C, their values were lower than those of SEBS (H1062). But, they became higher than SEBS (H1062) alone at temperatures higher than 80°C. The 50 wt % PS blends did not show any viscosity reductions from the value of neat SEBS. They exhibited the increases in both G' and complex viscosity, which were higher than those of SEBS (H1062) and approaching to those of PS. The blend of PS with SEBS (H1043) did not reduce G'

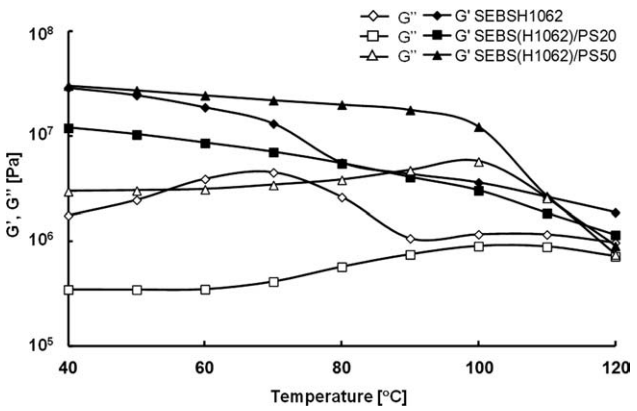

Figure 6. G' and G'' of SEBS (H1062) and their blends with PS.

from the value of SEBS (H1043) alone at any temperatures or any investigated blend ratios. G' value of SEBS (H1043)/PS blends slightly increased as the amount of PS increased in the range of 90 to 100°C, as shown in Figure 7.

To confirm that the viscosity of the SEBS (H1062)/PS (80/20) blend reduces at temperatures below 80°C and increases at a temperature of 100°C, the frequency dependency of the storage and loss moduli was measured at both 60 and 100°C for SEBS (H1062) alone and its blends. Figure 8(a, b) shows the G' and G'' of the SEBS (H1062) and blends as a function of frequency at 60 and 100°C. The storage moduli, G' of SEBS (H1062)/PS (80/20) blend decreased slightly at 60°C, but it became larger than the value of SEBS (H1062) alone at 100°C. Furthermore, at 60°C, the 50 wt % PS-blended samples exhibited slight

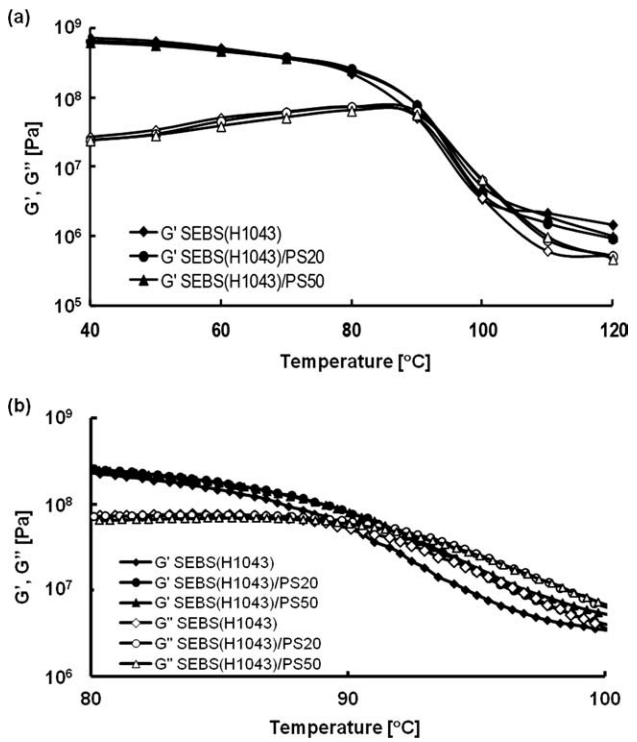

Figure 7. G' and G'' of SEBS (H1043) and their blends with PS.

increase in G' at low frequency, which resembles the behavior of a cross-linked polymer.

The polymer chain of SEBS consists of styrene and EB blocks. The micro-phase separation occurs and forms sea-island morphology, where the end segment (styrene block) forms spherical domains in cubic ordering EB continuous phase.[28] Wang et al.[29] claimed that high interfacial tension between styrene and EB blocks brings about the micro-phase separation. In 80/20 SEBS (H1062)/PS blend, due to interaction between styrene block of SEBS and PS polymer, the sea-island morphology was still formed but the size of styrene disperse domain seemed to increase slightly [Figure 9(b)] comparing with the disperse domain in EB continuous matrix in 50/50 blend [Figure 9(c)]. The slight increase in size of the styrene-disperse domain could reduce the G' and G'' values at 80/20 SEBS (H1062)/PS blend from those of SEBS (H1062) alone at temperatures below 80°C.

As observed, the 80/20 SEBS (H1062)/PS blend did not show so much difference in the CO_2 solubility and diffusivity from those of SEBS (H1062) alone. This might be caused by preservation of micro-phase separation in the blend.

When the added PS content increased to 50 wt % in the blend, the aggregation behavior of PS progressed, the size of PS

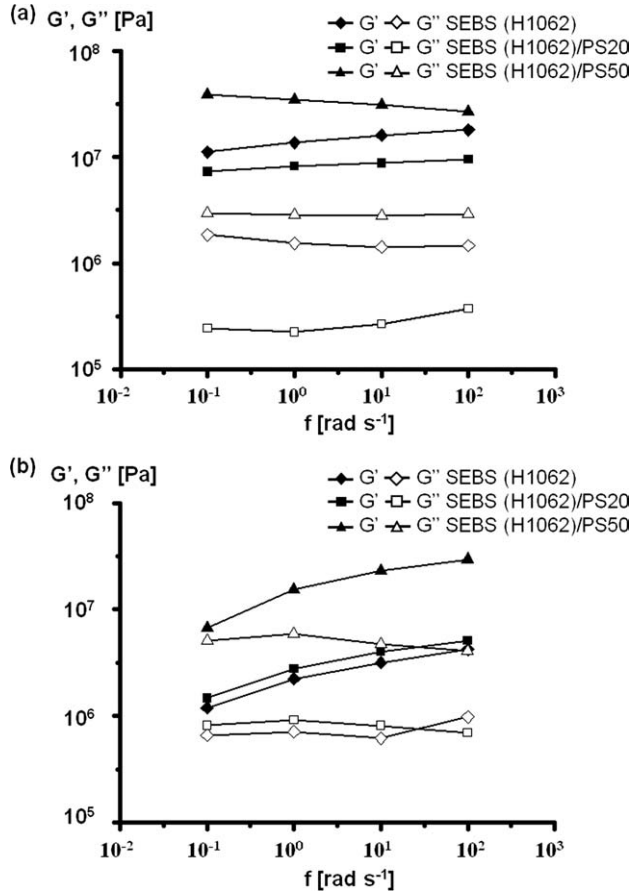

Figure 8. Frequency sweep measurement for SEBS (H1062) and 80/20 and 50/50 SEBS blends with 0.1% strain at different temperatures: (a) 60°C and (b) 100°C.

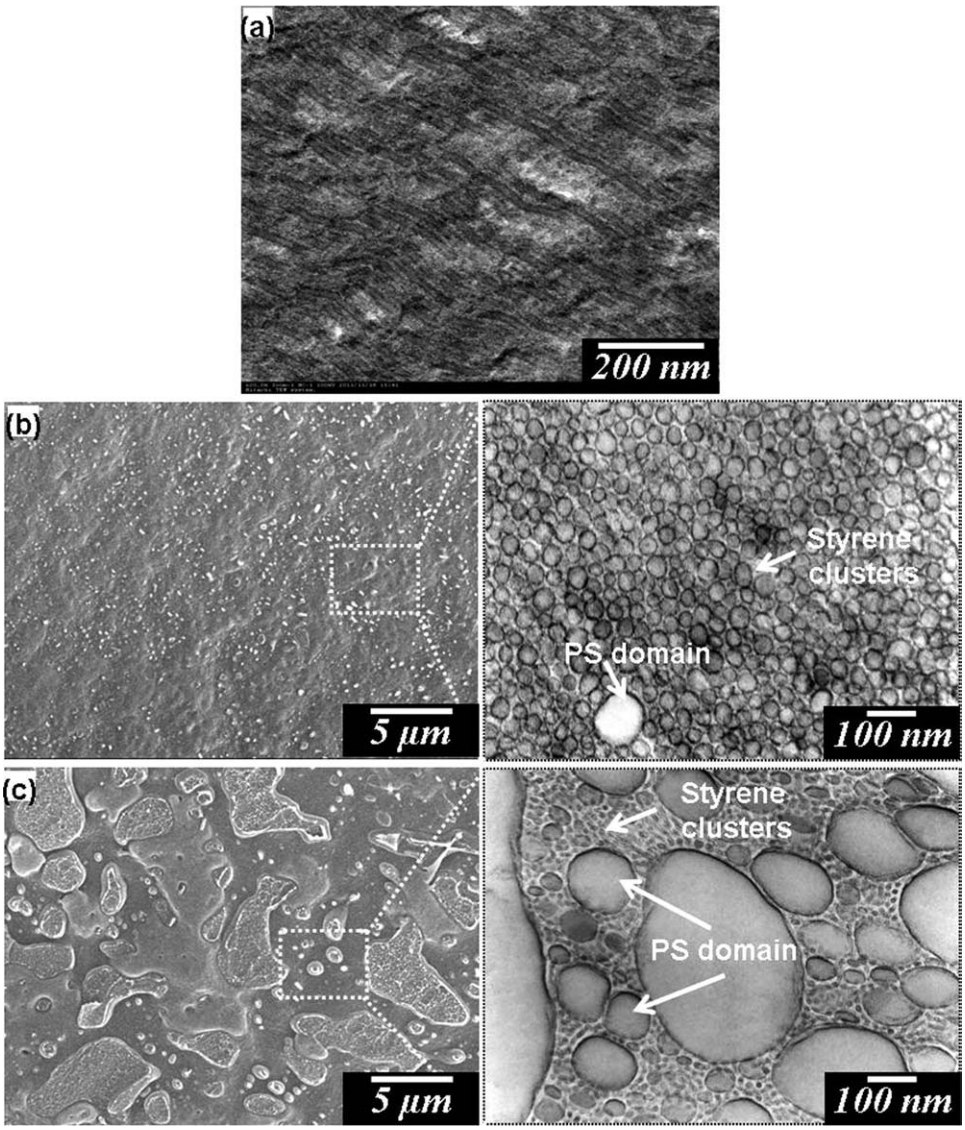

Figure 9. Blend morphologies of SEBS (H1062) and its blends: (a) SEBS (H1062), (b) SEBS (H1062)/PS (80/20), and (c) SEBS (H1062)/PS (50/50).

domain increased to micro-scale and the morphology changed from micro-phase separation to the morphology where PS formed micro-scale large domains as shown in Figure 9(c). Then, the effect of presence of stiff PS on viscosity would become stronger and viscosity increased at 50/50 SEBS (H1062)/PS blend.

Foaming Behavior of SEBS(H1062) and (H1043)

Figure 10 compares the cell structures of the foamed SEBS (H1062) and (H1043) alone. Three different foaming temperatures, 60, 100, and 155°C, were investigated under the same 10 MPa saturation pressure of CO_2. Both H1062 and H1043 were foamed. Their foam expansion ratios increased with the increase of the foaming temperature. SEBS (H1043) developed spherical pores, even though its foamability was not as high as that of SEBS (H1062). This effect was caused by the higher G' of SEBS (H1043). Because of the large dimensional instability with foam shrinkage, pores were not clearly observed in the SEBS (H1062) foams at any foaming temperatures, as shown in the images in the upper row of Figure 10.

Figure 11 shows the change in foam density as a function of time after the conclusion of foaming. After the SEBS copolymers were foamed at 60, 100, and 155°C, the foams were maintained at room temperature and atmospheric pressure, and the density of the foams was occasionally measured by the densimeter. The SEBS (H1062) foam exhibited a drastic increase in density over time (instability of foam) at 60°C. When the SEBS (H1062) was foamed at 155°C, the change in its density was too fast to be recorded, and the foam eventually exhibited a higher density (lower expansion ratio). This densification occurred because of the increase in the diffusivity and the decrease in G' with the increase of the foaming temperature. SEBS (H1062) was not rigid enough to prevent the foams from shrinking against the excess forces exerted by elastic deformation and the rapid gas loss from the cells.

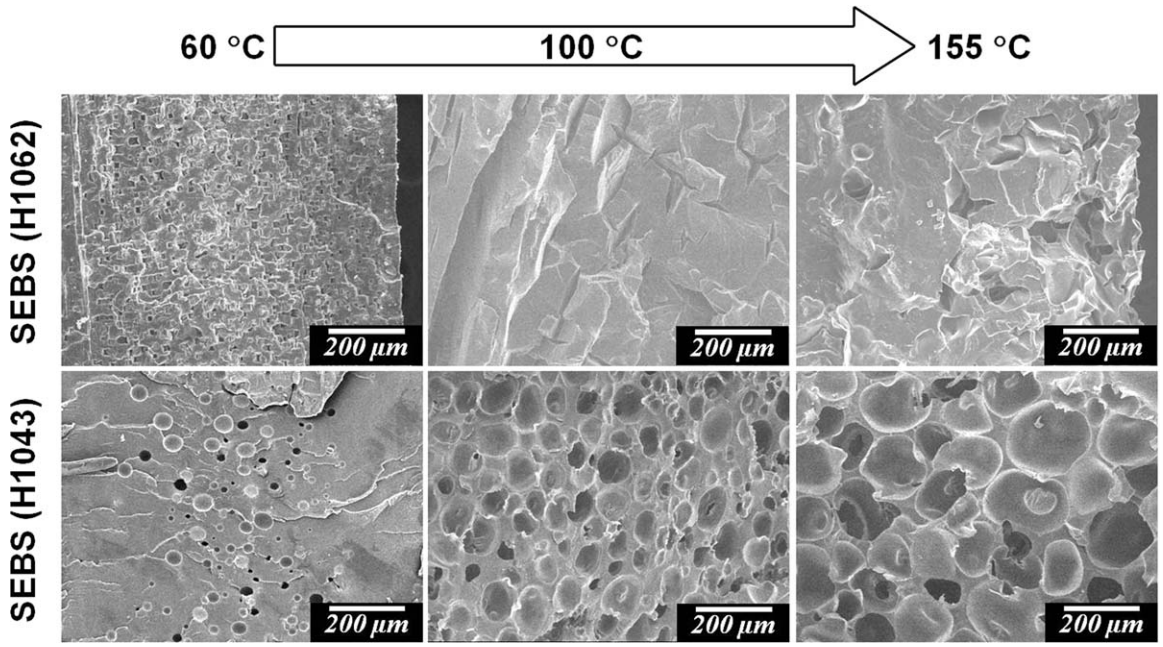

Figure 10. Cell structure of SEBS (H1062 and H1043) foams at three different temperatures: (a) 60°C, (b) 100°C, and (c) 155°C.

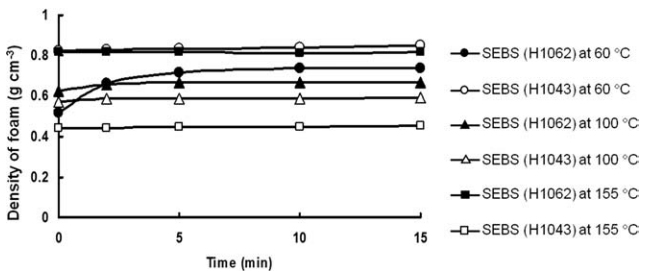

Figure 11. Shrinkage of SEBS (H1062 and H1043) foams (foam density-time curves).

In the SEBS (H1043) foams, the shrinkage was not as drastic as that of H1062 at both foaming temperatures. Because of the higher storage modulus, the expansion ratio was low at a foaming temperature of 60°C, but it was improved when the foaming temperature was increased to 155°C. The higher instability of the cell structure of the SEBS (H1062) foams could be explained by the higher diffusivity of CO_2 (Figures 3 and 4) and the lower storage modulus of the polymer (Figures 6 and 7). By comparison of the results of both H1062 and H1043, it can be observed that the increase in the styrene content of the SEBS decreased the CO_2 diffusivity and solubility while

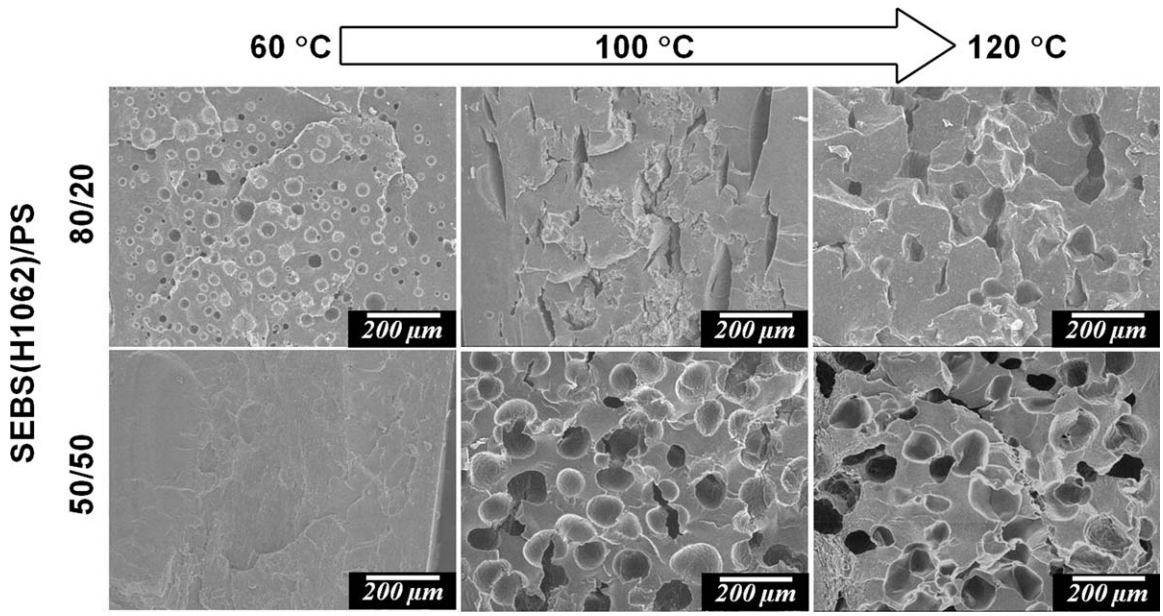

Figure 12. SEM micrographs of SEBS (H1062)/PS foams with weight ratios of 80/20 and 50/50 at different foaming temperatures.

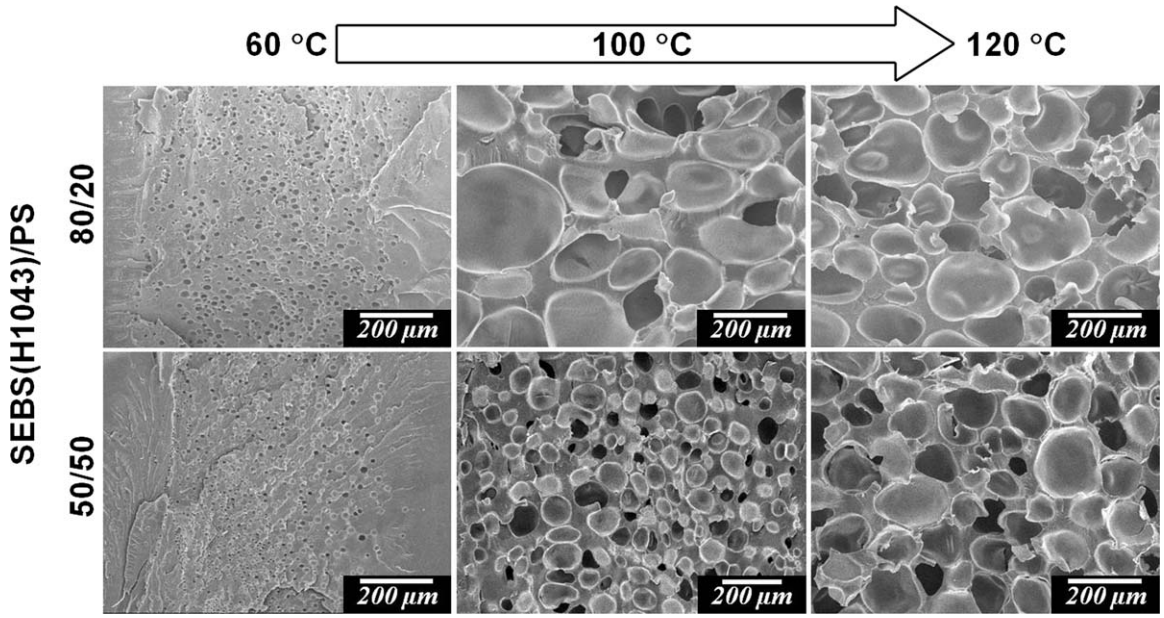

Figure 13. SEM micrographs of SEBS (H1043)/PS foams with weight ratios of 80/20 and 50/50 at different foaming temperatures.

simultaneously increasing the storage modulus and the complex viscosity, which stabilized the cell structure.

Foaming Behavior of SEBS/PS Blends

To control the storage modulus and CO_2 diffusivity, PS was blended with both SEBS copolymers. The SEBS (H1062)/PS and SEBS (H1043)/PS blends were prepared at different weight ratios (80/20 and 50/50) and foamed at different temperatures (60, 100, and 120°C). Figures 12 and 13 show SEM micrographs of the SEBS (H1062)/PS and SEBS (H1043)/PS blend foams, respectively. Figures 14 and 15 show the change in the foam density over time after foaming.

In the SEBS (H1062)/PS (80/20) foams, the cell size increased with elevated foaming temperature (Figure 12), but the foam density did not increase (Figure 14). As shown in Figure 14, the foam density (expansion ratio) reached its minimum (maximum) when the SEBS (H1062)/PS (80/20) was foamed at 100°C. The storage modulus and complex viscosity decreased with the increase of temperature, as shown in Figure 6. This viscosity reduction caused the cell growth to occur faster and the cell size to become larger. In addition, the CO_2 diffusivity increased as the temperature increased. These changes made the gas loss increase and reduced the expansion ratio at 120°C. By increasing the PS blend ratio to 50 wt %, the CO_2 diffusivity was lowered, as shown in Figure 4. Then, even though the foamability was not good at 60°C because of the higher storage modulus, it was improved by increasing the foaming temperature, as shown in Figures 12 and 14.

For the case of the SEBS (H1043)/PS foams, the cell size increased as the foaming temperature increased at blend ratios of both 80/20 and 50/50. The difference in the foaming behavior from that of the SEBS (H1062)/PS blends was induced by the lower CO_2 diffusivity and the higher storage modulus.

Blending PS with the SEBS produced a polymer matrix that was rigid enough to prevent the cell from shrinking.

CONCLUSIONS

This study showed the possibility of controlling the shrinkage of SEBS foams by increasing the styrene content or blending with PS. The styrene content strongly influenced the foaming behavior and cell structure. Greater styrene contents increased the storage modulus and reduced the CO_2 solubility and diffusivity. As a result, the cell structure was stabilized. The appropriate

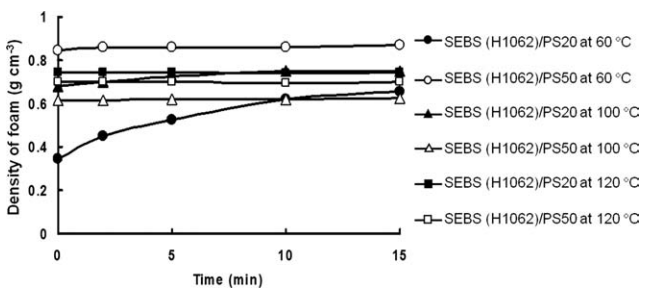

Figure 14. Shrinkage of SEBS (H1062)/PS with blend ratios of 80/20 and 50/50 at different foaming temperatures.

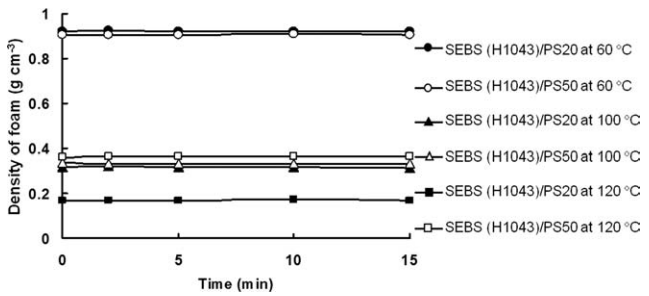

Figure 15. Shrinkage of SEBS (H1043)/PS with blend ratios of 80/20 and 50/50 at different foaming temperatures.

level of storage modulus to provide increased rigidity and reduced diffusivity led to a reduction of the shrinkage. This study can be extended to further investigate the effect of the length of the EB block in SEBS on the physical crosslink constructed between the SEBS and the PS.

ACKNOWLEDGMENTS

The authors would like to acknowledge the New Energy and Industrial Technology Development Organization (NEDO) for the financial support of the project for developing innovative nofluourocarbon-based heat insulation technology. University Technology MARA (UiTM) is also acknowledged for providing the scholarship to one of the authors.

REFERENCES

1. Najib, N. N.; Ariff, Z. M.; Bakar, A. A.; Sipaut, C. S. *Mater. Des.* **2011,** *32*, 505.
2. Sambatsomsop, N.; Lertkamsosin, P. *J. Elastomers Plast.* **2000,** *32*, 311.
3. Lawindy, A. M. Y. E. *Egypt. J. Sol.* **2002,** *25*, 295.
4. Kim, S. G.; Park, C. B.; Sain, M. *J Cell. Plast.* **2008,** *44*, 53.
5. Sahnoune, A.; *J. Cell. Plast.* **2001,** *37*, 149.
6. Kim, J. H.; Choi, K. C.; Yoon, J. M. *J. Ind. Eng. Chem.* **2006,** *12*, 795.
7. Gendron, R.; Vachon, C. *J Cell. Plast.* **2003,** *39*, 117.
8. Gendron, R.; Vachon, C. *J. Cell. Plast.* **2003,** *39*, 71.
9. Fan, R. L.; Zhang, Y.; Li, F.; Zhang, Y. X.; Sun, K.; Fan, Y. Z.; *Polym. Test.* **2001,** *20*, 925.
10. Tai, H. J. *J. Polym. Res.* **2005,** *12*, 457.
11. Ariff, Z. M.; Zakaria, Z.; Tay, L. H.; Lee, S. Y.; *J. Appl. Polym. Sci.* **2008,** *107*, 2531.
12. Giri, R.; Sureshkumar, M. S.; Naskar, K.; Bharadwa, Y. K.; Sarma, K. S. S.; Sabhrwal, S.; Nando, G. B. *Adv. Polym. Tech.* **2008,** *27*, 99.
13. Ahmed, F. S.; Shafy, M.; El-Megeed, A. A. A.; Hegazi, E. M. *Mater. Des.* **2012,** *36*, 823.
14. Liu, P.; Liu, D.; Zhou, H.; Fan, P.; Xu, W. *J. Appl. Polym. Sci.* **2009,** *113*, 3590.
15. Dubey, K. A.; Bhardwaj, Y. K.; Chaudhari, C. V.; Bhattacharya, S.; Gupta, S. K.; Sabharwal, S. *J. Polym. Sci.* **2006,** *44*, 1676.
16. Lin, H.; Alkadasi, N. A. N.; Zhu, Y.; Tong, L. F.; Fang, Z. P.; Wang, Y. C. *Front. Mater. Sci. China* **2008,** *2*, 426.
17. Banik, I.; Bhowmick, A. K.; Raghavan, S. V.; Majali, A. B.; Tikku, V. B. *Polym. Degrad. Stabil.* **1999,** *63*, 413.
18. Pikaev, A. K. *High Energy Chem.* **2002,** *36*, 135.
19. Chaudhari, C. V.; Dubey, K. A.; Bhardwaj, Y. K.; Naxane, G.; Sarma, K. S. S.; Sabharwal, S. *Nuclear Instr. Methods Phys. Res. B* **2007,** *263*, 451.
20. Zhai, W.; Leung, S. N.; Wang, L.; Naguib, H. E.; Park, C. B. *J. App. Polym. Sci.* **2010,** *116*, 1994.
21. Areerat, S.; Hayata, Y.; Katsumoto, R.; Kegasawa, H.; Egami, H.; Ohshima, M. *J. Appl. Polym. Sci.* **2002,** *86*, 282.
22. Sanchez, I. C.; Lacombe, R. H. *Macromolecules* **1978,** *11*, 1145.
23. Sato, Y.; Takikawa, S.; Masuoka, H. *J. Supercrit. Fluids* **2001,** *19*, 187.
24. Areerat, S.; Funami, E.; Hayata, Y.; Nakagawa, D.; Ohshima, M. *Polym. Eng. Sci.* **2004,** *44*, 1915.
25. Li, Y. G.; Park, C. B.; Li, H. B.; Wang, J. *Fluid Phase Equilibria* **2008,** *270*, 15.
26. Funami, E.; Taki, K.; Ohshima, M. *J. Appl. Polym. Sci.* **2007,** *105*, 3060.
27. Kaplan, W. A.; Tabor, R. L. *J. Reinforced Plast. Compos.* **1994,** *13*, 155.
28. Peinado, C.; Corrales, T.; Catalina, F.; Pedron, S.; Quiteria, V. R. S.; Parellada, M. D.; Barrio, J. A.; Olmos, P.; Benito, J. G. *Polym. Degrad. Stabil.* **2010,** *95*, 975.
29. Wang, L.; Zhao, J.; Han, C. C. *Polymer* **2008,** *49*, 2153.